SUMO Modification Stabilizes Enterovirus 71 Polymerase 3D to Facilitate Viral Replication

Yan Liu[1], Zhenhua Zheng[1#], Bo Shu[1], Jin Meng[1], Yuan Zhang[1], Caishang Zheng[1], Xianliang Ke[1], Peng Gong[1], Qinxue Hu[2], Hanzhong Wang[1]

1. Key Laboratory of Special Pathogens and Biosafety, Center for Emerging Infectious Diseases, Wuhan Institute of Virology, Chinese Academy of Sciences, Wuhan 430071, China

2. State Key Laboratory of Virology, Wuhan Institute of Virology, Chinese Academy of Sciences, Wuhan 430071, China

[#]Corresponding author: Dr. Zhenhua Zheng, E-mail: zhengzh@wh.iov.cn

Running title: SUMOylation of EV71 3D Facilitates Viral Replication

Word count: Abstract (237 words) Text (6143 words)

Abstract

Accumulating evidences suggest that viruses hijack cellular proteins to circumvent the host immune system. Ubiquitination and SUMOylation are extensively studied post-translational modifications (PTMs) that play critical roles in diverse biological processes. Crosstalk between ubiquitination and SUMOylation of both host and viral proteins has been reported to result in distinct functional conses1quences. Enterovirus 71 (EV71), an RNA virus belonging to *Picornaviridae* family, is a common cause of hand, foot and mouth disease. Little is known concerning how host PTM systems interact with enteroviruses. Here, we demonstrated that the 3D protein, an RNA-dependent RNA polymerase (RdRp) of EV71, is modified by small ubiquitin-like modifier-1 both during infection and *in vitro*. Residues K159 and L150/D151/L152 were responsible for 3D SUMOylation determined by bioinformatic prediction combined with site-directed mutagenesis. And primer-dependent polymerase assays indicated that mutation of SUMOylation sites impaired 3D polymerase activity and virus replication. Moreover, 3D is ubiquitinated in a SUMO-dependent manner, and SUMOylation is crucial for 3D stability which may be due to the interplay between the two PTMs. Of importance, increasing the level of SUMO-1 in EV71-infected cells augmented the SUMOylation and ubiquitination level of 3D, leading to enhanced replication of EV71. These results together suggested that SUMO and ubiquitin cooperatively regulated EV71 infection either by SUMO-ubiquitin hybrid chains or by ubiquitin conjugating to the exposed lysine residue through SUMOylation. Our study provides a new insight into how a virus

35 utilizes cellular pathways to facilitate its replication.

36

Importance

Infection with Enterovirus 71（EV71）often causes neurological diseases in children and EV71 is responsible for the majority of fatalities. Based on a better understanding of interplay between virus and host cell, antiviral drugs against enteroviruses may be developed. As a dynamic cellular process of post-translational modification, SUMOylation regulates global cellular protein localization, interaction, stability, and enzymatic activity. However, little is known concerning the SUMOylation directly influence virus replication by targeting viral polymerase. Herein, we found that EV71 polymerase 3D was SUMOylated during EV71 infection and *in vitro*. Moreover, the SUMOylation sites were determined. And *in vitro* polymerase assays indicated that mutations at SUMOylation sites could impair polymerase synthesis. Importantly, 3D is ubiquitinated in a SUMOylation-dependent manner which enhances the stability of the viral polymerase. Our findings indicate that the two modifications likely cooperatively enhance virus replication. Our study may offer a new therapeutic strategy against virus replication.

Introduction

Small ubiquitin-like modifier (SUMO) modification, a member of post-translational modifications (PTMs), is important for the regulation of many cellular proteins and pathways (1). SUMO represents a novel protein modifier similar to the well-studied ubiquitin. Structural analysis revealed high similarities between the two PTMs despite limited (18%) sequence identity (2). Four SUMO isoforms exist in vertebrates with each having an approximate molecular mass of 12 kDa. SUMO-2 and SUMO-3 can form polymeric SUMO chains via a single, conserved lysine residue (3, 4). Without such site, SUMO-1 cannot act as a linkage to elongate chains *in vivo* but as a chain terminator on poly-SUMO-2, 3 chains (5-7).

Similar to ubiquitination, SUMO proteins are initially synthesized as inactive precursors and cleaved by a specific protease belonging to the family of sentrin-specific proteases (SENPs) to expose the COOH-terminal diglycine motif (8). The carboxyl terminus of mature SUMO peptide is linked to a cysteine residue in E1-activating enzyme (SUMO-activating enzyme, SAE1/SAE2) via a thioester in an ATP-dependent manner. The activated SUMO is subsequently transferred to a cysteine residue of the SUMO-conjugating enzyme Ubc9. Although Ubc9 can transfer SUMO to the target protein, mutual action of Ubc9 and E3 SUMO ligases is required for an efficient modification (9-11). An isopeptide bond is formed between the lysine residue of the target protein and SUMO. The modification is dynamically reversible. In addition to its role in SUMO precursor maturation, SENPs also act as SUMO

74 deconjugation enzymes to complete the SUMO modification (SUMOylation) cycle
75 (8).

76 Typically, the lysine in the amino acid consensus motif ψ-K-X-D/E or inverted motif
77 E/D-X-K-ψ (ψ represents a large hydrophobic residue) of a protein is recognized as
78 SUMOylation site (6, 12, 13). Apart from covalent modification, target proteins may
79 be modified non-covalently via SUMO-interacting motifs (SIMs) (6, 12). In general,
80 the SIMs contain a hydrophobic core (V/I-x-V/I-V/I or V/I-V/I-x-V/I/L), flanked by
81 acidic residues either upstream or downstream (14-17). In addition to being
82 structurally related, ubiquitin and SUMO modification of substrates are preferentially
83 occurring on lysine residues, and ubiquitin can be hybridized with SUMO moiety by
84 anchoring to the lysine on poly-SUMO (18, 19). Crosstalk between the two PTMs
85 may be involved in genome stability and cell growth, which are associated with
86 pathogen resistance and cancer treatment (20). Studies indicate that SUMOylation can
87 antagonize ubiquitin/proteasome mediated degradation by competing the same lysine
88 to stabilize the target protein or cooperatively degrade the target protein by sharing the
89 same lysine with ubiquitin (20, 21).

90 Viruses, as obligate pathogenic organisms, must usurp the host proteins and cellular
91 pathways throughout their life cycles to evade antiviral defenses by creating an
92 environment that facilitates their replication (7). Many viral proteins have been
93 identified as substrates for SUMOylation. Viruses can interact with and exploit the
94 enzymes of the SUMO pathways to promote their assembly, replication, or to evade

the host immune system. Viruses could also be constrained by the host SUMO systems and vice versa (22). Some viruses possess more than one SUMOylated proteins, indicating the complexity of virus-host interactions. For instance, SUMOylation of cytomegalovirus (HCMV) DNA polymerase subunit UL44, and immediate-early 1 and 2 proteins (IE1 and IE2) are required for an efficient viral replication (23-26). At least five influenza virus proteins are SUMO targets, and the infection of influenza virus leads to a global increase in cellular SUMOylation (27). SUMOylation of NS1 accelerates virus growth; M1 protein SUMOylation facilitates viral ribonucleoprotein export and the assembly of virus particles; and NP protein SUMOylation regulates the intracellular trafficking of NP and efficient virus production (28-30). The early lytic gene product (K-bZIP), the major transcriptional factor (K-Rta), and the latency-associated nuclear antigen 2 of Kaposi's sarcoma-associated herpesvirus are SUMOylated to achieve an efficient viral replication (31-33). SUMOylation of the p6 domain of Gag polyprotein and integrase of human immunodeficiency virus type 1 are important for virus replication (34, 35). Nevertheless, SUMOylated viral proteins from other viruses remain to be discovered. A global study of viruses and host SUMOylation will enhance our understanding of the interactions between viruses and the host.

EV71 belongs to the *Enterovirus* genus (human *Enterovirus* A) of the *Picornaviridae* family, which causes severe neurological diseases in young children under five years old, known as hand, foot and mouth disease (36). Similar to other human *Enterovirus*, including Poliovirus, Coxsackie virus, and Echovirus, EV71 is a single-stranded RNA

117 virus with a single open reading frame encoding a precursor protein. After infection,
118 the precursor is cleaved into four structural (VP1, VP2, VP3, and VP4) and seven
119 nonstructural (2A, 2B, 2C, 3A, 3B, 3C, and 3D) proteins (37). The 3D protein is a
120 RNA-dependent RNA polymerase ($3D^{pol}$) and responsible for the process of RNA
121 replication. 3C protease is SUMOylated at lysine residue 52 (K52) by SUMO-1.
122 SUMOylation of 3C increases ubiquitination, which leads to the degradation of 3C
123 and eventually causes the reduction of viral replication (38). Our bioinformatic
124 analysis suggested that EV71 3D polymerase is likely to be SUMOylated and may
125 contain both covalent and non-covalent motifs. However, whether 3D is indeed
126 SUMOylated and the role of such modification during the infection remain to be
127 addressed.

128 In the present study, we demonstrated that EV71 3D is modified by SUMO-1 both *in*
129 *vivo* and *in vitro*. We further identified K159 and 150-152 SIM as the sites for
130 SUMOylation. Mutations at both SUMOylation sites impaired polymerase synthesis
131 in *in vitro* polymerase assays. In addition, we found that the K63-linked ubiquitin
132 modification of 3D is SUMOylation-dependent, and a combination of the two
133 modifications resulted in higher 3D stability and enhanced viral replication. Although
134 SUMOylation of 3C and 3D resulted in opposite effects on virus reproduction,
135 enhanced EV71 replication in SUMO-1-elevated cells indicates that 3D SUMOylation
136 plays a predominant role. Our findings together imply that EV71 exploits host cellular
137 modification for effective replication, revealing a potential target for antiviral therapy.

Materials and methods

Cell culture and virus manipulation

Human embryonic kidney cells (HEK 293T) (China Center for Type Culture Collection, CCTCC) and African green monkey kidney epithelial cell (Vero, CCL-81, American Type Culture Collection) were cultured in Dulbecco's Modified Eagle Medium. Human rhabdomyosarcoma cell (RD, CCL-136, American Type Culture Collection) were grown in Minimal Essential Medium. All cells were maintained in medium containing 10 % fetal bovine serum (Life Technology, Australia) in 5 % CO_2 at 37 °C.

EV71 BrCr strain was obtained from the Institute of Medical Biology, Chinese Academy of Medical Science (39). Virus titers were measured by 50 % tissue culture infectious dose (TCID50) in RD cells using the Reed–Muench formula (40). One step growth curve of viruses were determined with parental EV71 at a desired multiplicity of infection (MOI) (41). EV71 infectious clone was kindly provided by Minetaro Arita (National Institute of Infectious Diseases, Tokyo, Japan) (42). EV71 infectious clone and its mutant recombinant RNAs were *in vitro* transcribed by RiboMAX large-scale RNA production system-T7 kit (Promega) (43). The RNAs were transfected into Vero cells to rescue EV71 wild-type and mutant viruses, and these viral strains were amplified in RD cells (39).

Antibodies and reagents

158 EV71 3D, 3C, and VP1 polyclonal antibodies were prepared by immunizing rabbits
159 with His tag-3D, 3C, and VP1 fusion proteins, respectively. Rabbit anti-hemagglutinin
160 (HA) and mouse anti-V5 antibodies were purchased from CoWin Biotech (Beijing,
161 China). Mouse anti-β-actin antibody was acquired from Proteintech (Wuhan, China).
162 Rabbit anti-SUMO-1, 2, and 3 antibodies were purchased from Cell Signaling
163 Technology (Beverly, MA, USA). Mouse monoclonal anti-flag M2 and mouse
164 anti-HA antibodies were purchased from Sigma–Aldrich (St Louis, MO). Mouse
165 anti-myc, mouse monoclonal anti-Ub, and mouse control IgG were obtained from
166 Abmart (Shanghai, China), Santa Cruz (CA, USA), and Boster (Wuhan, China),
167 respectively. MG132, a proteasome inhibitor, and complete protease inhibitor cocktail
168 were purchased from Calbiochem (San Diego, CA, USA) and Roche (Roche,
169 Indianapolis, IN), respectively. *N*-Ethylmaleimide (NEM) and cycloheximide (CHX)
170 were obtained from Sigma-Aldrich. Western and IP lysis buffer and RIPA lysis buffer
171 were purchased from Beyotime (Jiangsu, China).

172 **Plasmid construction**

173 Flag-3D and HA-3D were generated by inserting EV71 3D coding sequence into
174 pCAGGS as previously described (44, 45). All the mutations of 3D (K159R,
175 L150A/D151A, L150A/D151A/L152A, K159R/L150A/D151A/L152A,
176 V263A/S264A/L265A, and I317A/D318A/L319A) were created by overlapping
177 extension PCR. Recombinant EV71 harboring 3D mutations were constructed by
178 overlapping extension PCR using the infectious clone as a template at indicated sites.

179 The verification of the mutants was performed by RNA extraction, reverse
180 transcription and PCR (39).

181 pcDNA3-HA-SUMO-1 was obtained from Junying Yuan (Addgene plasmid 21154)
182 (46). SRa-HA-SUMO-2, pcDNA3/HA-SUMO-3, and Flag-SENP-1 were gifts from
183 Edward Yeh (Addgene plasmid 17360, 17361, and 17357) (47, 48). pCMV hUbc9 wt
184 HA was a gift from Peter Howley (Addgene plasmid 14438) (49).
185 pcDEF-HA-SUMO-1, pcDEF-Myc-Ubc9, and pcDEF-Flag-SUMO-2 were
186 generously provided by Hong Tang (Wuhan Institute of Virology, Chinese Academy
187 of Sciences, Wuhan, China) (50). pRK-Flag-SUMO-2 was kindly provided by Yanyi
188 Wang (Wuhan Institute of Virology, Chinese Academy of Sciences, Wuhan, China)
189 (51). Myc-SUMO-1 and V5-SENP-1 were constructed by inserting SUMO-1 and
190 SENP-1 coding sequences into pCAGGS, respectively. Flag-SUMO-1, 2, and 3 were
191 created by amplifying and inserting their coding sequences into pCAGGS.
192 HA-K48-Ub and HA-K63-Ub were mutants of HA-Ub with all lysine residues
193 mutated into arginines, except K48 and K63 (52). HA-UB-(KO) was a mutant of
194 ubiquitin created by the substitution of lysine residues Lys63 of HA-K63-Ub with
195 arginine.

196 The plasmid expressing wild-type (WT) 3D was generated by cloning the 3D gene
197 into a pET26-Ub vector (53, 54), and the 3D K159R, K159A, and L150A/D151A
198 mutants were further constructed using the WT plasmid as the template. 3D was
199 cloned into pGEX-6p-1 (GE Healthcare) to produce GST-tag 3D. pSUMO-1

containing SUMO-activating enzyme E1 (SAE1 and SAE2) was from Primo Schär (Addgene plasmid 52258) (55). His-tag in pSUMO-1 was substituted with Strep-tag to create a pSUMO-1-Strep.

Protein preparation and *in vitro* polymerase assays

The plasmids for the expression of WT 3D and its variants were transformed into *Escherichia. coli* strain BL21 (DE3) (pCG1) (kindly supplied by Dr. Craig Cameron) for expression (54). The bacteria were cultured and purified as described previously, except that the induction condition before harvesting was 11 h at 25 °C (56). The preparation of the 33-nucleotide RNA template (T33) was as described previously (57, 58). The 10-nucleotide RNA primer (P10) was purchased from Integrated DNA Technologies. The T33/P10 construct was annealed at 45 °C for 3 min at a molar ratio of 1:0.9 in an RNA annealing buffer (RAB) (50 mM NaCl, 5 mM Tris [pH 7.5], 5 mM $MgCl_2$). A typical 20 µl reaction mixtures containing 6 µM 3D or its mutants, 50 mM Tris [pH 7.0], 20 mM NaCl, 55 mM KCl, 5 mM $MgCl_2$, 4 mM TCEP (tris-[2-carboxyethyl]phosphine), 300 µM ATP, 4 µM (T33/P10) construct and 300 µM GTP were incubated at 22.5 °C for 15, 30, or 60 min before being quenched by an equal volume of stop solution (95 % [vol/vol] formamide, 20 mM EDTA [pH 8.0], 0.02 % [wt/vol] bromphenol blue, and 0.02 % [wt/vol] xylene cyanol). The quenched samples were heated at 100 °C for 3 min. The RNA species in the reaction mixture were resolved by 20 % polyacrylamide–7 M urea gel electrophoresis before staining with Stains-All (Sigma–Aldrich). Color images obtained by scanning the stained gels

were converted to grey-scale images prior to quantification by Image J (http://imageJ.nih.gov/ij/). The Stains-All-based quantification method was used previously to assess the amount of RNA with similar lengths (58).

In vitro SUMOylation assay

The SUMOylated 3D proteins were produced by introducing pGEX-6p-3D into *Escherichia coli* (E.coli) BL21 (DE3) harboring pSUMO-1-Strep by electroporation. Strains were grown under selective pressure at 50 mg/L ampicillin and 25 mg/L streptomycin for co-expressing the two plasmids. The bacterial strains were cultured, and the protein was purified as previously described in the purification of 3D (53, 59), except that cell lysates were first loaded on GSTrap HP column (GE Healthcare, Waukesha, WI, USA). Subsequently, the eluted fractions were passed through StrepTrap HP column (GE Healthcare, Waukesha, WI, USA). After the two steps of enrichment, the extractions were separated by anion exchange and size exclusion chromatography for further purification (55). The collected fractions were electrophoresed on SDS-polyacrylamide gel (SDS-PAGE) detected by Coomassie blue staining or immunoblotting using Bio-Rad Imaging System. The immunoblot analysis was performed as previously described (45).

SUMOylation and Ubiquitination assays

SUMOylation and ubiquitination assays were performed with Dynabeads protein G (Life Technology, Grand Island, NY) for immunoprecipitation (IP). 293T cells were

241 cotransfected with indicated plasmids using calcium phosphate reagents of ProFection
242 (Promega, Southampton, UK). For the assay of ubiquitination, 30 h post-transfection，
243 cells were lysed with western and IP lysis buffer plus complete protease inhibitors
244 according to the manufacturer's instructions. For the SUMOylation assay, after 30 h of
245 transfection, cells were harvested and lysed with western and IP lysis buffer plus
246 complete protease inhibitors and 20 mM NEM. The lysates were centrifuged at
247 16,000 g at 4 °C for 10 min. According to the protocol, 10 μg of corresponding
248 antibody was incubated with 50 μL of protein G Dynabeads for 20 min before
249 incubation with the supernatants of the cell lysis for 25 min. Following several washes
250 with PBST (PBS with 0.02 % Tween-20), the complexes were boiled with
251 electrophoresis sample buffer, followed by immunoblot (IB) analysis with indicated
252 antibodies as previously described (45, 52).

253 In assays involved EV71 infection, cells were cultured on 100-mm dishes. At 24 h
254 post-transfection, 293T cells were infected with EV71 at an MOI of 10 for 18 h before
255 harvesting. For the infection of RD, cells were lysed with RIPA lysis buffer after
256 infection with EV71 at an MOI of 10 for 8 h. The supernatants were collected for IP
257 as describe above.

258 **CHX chase analysis**

259 The CHX chase experiment was performed as described in Bio-protocol (60). Cells
260 were seeded on 35 mm culture dishes at a density of 6×10^6 cells. Cells were
261 transfected with Flag-3D and its mutant Flag-K159R/L150A/D151A/L152A. After 24

h, cells were treated with 100 μg/mL of CHX dissolved in DMSO in the presence or absence of 20 μM MG132. Cells were then collected at different time points and subjected to immunoblots. The quantification of protein levels was analyzed by Image J software.

Statistical analysis

Each of the experiment was repeated at least three times. Data from viral titer, one step growth curve, primer-dependent polymerase assays and CHX chase are presented as the mean ± standard deviation. Student's *t*-test was used to determine the statistical significance between different tests, with significance defined as $P < 0.05$ or $P < 0.01$.

Results

3D polymerase is SUMOylated during EV71 infection

SUMOylation is one of the post-translational modifications (PTMs) that play critical roles in diverse biological processes. However, little is known concerning how host PTM systems interact with enteroviruses 71. Online prediction suggested that EV71 3D polymerase may bear SUMOylation sites. Herein, we performed experiments to investigate the SUMOylation of 3D during EV71 infection. RD cells infected with EV71 were harvested at 8 h post-infection before immunoprecipitating with an anti-3D antibody. Structural proteins VP1 and 3D polymerase of EV71 were detected in cell lysates, and the anti-3D antibody was able to detect 3D and its precursors 3BCD and 3CD (Fig. 1B). SUMOylation and ubiquitination of 3D were detected by

anti-SUMO-1 antibody and anti-Ub antibody (Fig. 1A). Notably, IP by anti-3D antibody could obtain 3D, 3CD, and 3BCD complexes, whereas 3C was proven to be SUMOylated, bands detected by anti-SUMO-1 antibody might be a mixture of 3D SUMOylation, 3CD SUMOylation and 3BCD SUMOylation. Anti-3C antibody only detected protein 3CD (about 73 kDa), anti-3D antibody detected both 3CD and SUMOylated 3D, and anti-SUMO-1 antibody detected SUMOylated bands (Fig. 1A). The bands detected by anti-3C antibody was different from that by anti-SUMO-1 antibody or by anti-3D antibody, excluding the influence of 3CD and 3BCD SUMOylation (Fig. 1A). The SUMOylated 3Dpol was depicted by asterisks in the western blot detected by IP anti-3D followed by anti-SUMO-1 and anti-3D. The result of anti-SUMO-1 antibody showed one more SUMOylated band than that of anti-3D antibody, and this might be due to the antigenic epitope limitation of anti-3D antibody. Altogether, these results confirmed that EV71 3D could be SUMOylated during infection.

EV71 3D is modified by SUMO-1 and 3

We then performed experiments to confirm the SUMOylation of EV71 3D. SUMOylation is reversible by SENPs, which could be irreversibly inhibited by NEM; hence, the successful detection of this modification relies on the addition of NEM in the lysis buffer. We designed two experiments (Fig. 2A and 2B). Flag-3D, HA-SUMO-1, and Myc-Ubc9 (SUMO E2-conjugating enzyme) were overexpressed in 293T cells. At 30 h post-transfection, the cells were subjected to

303 immunoprecipitation with anti-Flag antibody. Higher molecular weights bands above
304 unmodified 3D (~52 kD) ranging within 80–130 kD were detected by an
305 anti-SUMO-1 or anti-HA antibody in the presence of NEM (Fig. 2A). The basal
306 SUMO-1 moiety of 3D was removed when co-expressed with SENP-1 (Fig. 2B). For
307 further verification, we performed co-immunoprecipitation experiment to study the
308 relationship between 3D and Ubc9 with an anti-Flag antibody. The result showed that
309 the SUMO-conjugating enzyme Ubc9 was present in the immunoprecipitated
310 complex (Fig. 2C), indicating that 3D could interact with Ubc9. Furthermore, when
311 3D was co-expressed with SUMO-1, 2, and 3 in 293T cells, 3D was preferentially
312 modified by SUMO-1 and 3 in poly-SUMO chain conjugation, which could be
313 deSUMOylated by SENP-1 (Fig. 2D).

314 **K159 and L150/D151/L152 are responsible for the SUMOylation of EV71 3D**

315 SUMO-1 conjugation has been reported to bind virtually to target proteins to regulate
316 physiological processes, whereas SUMO-2 and 3 are more widely expressed as free
317 non-conjugated forms, which are available for stress responses (22, 61).
318 Unconjugated pool of SUMO-1 is lower than that of SUMO-2 and 3 (62), therefore
319 our study focused on SUMO-1 modification. Bioinformatics analysis by SUMOplot
320 Analysis Program predicted that several lysine residues in 3D may be modified by
321 SUMO. K159, K376, and K427 of 3D following the consensus motif of ψ-K-X-D/E
322 are the top three lysine residues on the list (Fig. 4A). K323 fits the inverted
323 SUMOylation consensus motif E/D-x-K-ψ (Fig. 4A). The four lysine residues were

mutated to arginines to create mutants K159R, K376R, K427R and K323R. 3D and its mutants were co-expressed with SUMO-1 and Ubc9 in 293T cells to perform SUMOylation assays. Immunoprecipitation experiments indicated that the K323R, K376R, and K427R mutants had no obvious effect on SUMO-1 reduction, whereas K159R largely abolished the larger migration bands above 90 kD (Fig. 3A). These results also indicated that there are likely to be more than one site existed besides K159, which could be modified.

As depicted above, SIMs are featured by hydrophobic amino acid cores flanked by acidic residues (V/I)(V/I)(D/E)(V/I/L)(T/D/E) and (V/I)(V/I)(V/I/L)(V/I/L)(D/E) (14, 17). We created three mutants of 3D, namely, 150-152 SIM and 317-319 SIM which were created through inspecting 3D amino acid sequence, and 263-265 SIM which was predicted by SUMO-binding motif online prediction website (GPS-SBM) (Fig. 4A) (63). Three alanines were introduced to substitute the LDL, VSL, and IDL of the SIMs to create the mutants. Fig. 3B shows that the band modified by SUMO-1 around 80 kDa was considerably decreased in 150-152 SIM, whereas 263-265 SIM maintained almost the same bands as the wild-type 3D. 317-319 SIM completely attenuated the modified bands which was likely due to protein reduction in lysis. Considering the characteristics of the mutants, we constructed a mutant K159R/150-152 SIM by combining the mutation of K159R and 150-152 SIM. This mutant had remarkably decreased SUMO-1 modification in comparison with 3D or K159R, and 150-152 SIM (Fig. 3C). In the assay of SUMO-3, K159R lost the bands above 90 kDa, and K159R/150-152 SIM almost lost the SUMOylation totally, which

346 were similar to those in SUMO-1 (Fig. 3D). These results indicated that SUMO-3
347 modification of 3D shares the same sites with SUMO-1. Furthermore, single mutation
348 on K159 resulted in the reduction of higher bands but not the band around 80 kDa in
349 the assay with both SUMO-1 and SUMO-3 (Fig. 3C, 3D), indicating that position 159
350 was first modified by SUMO-3 and subsequently by SUMO-1 into a
351 poly-SUMOylated chains. These results were observed because SUMO-1 could not
352 be elongated and always acts as a terminator of ploy-SUMO chains (6, 7). In
353 conclusion, K159 and L150/D151/L152 may be responsible for the SUMOylation of
354 EV71 3D.

355 **Mutations of SUMOylation sites impair 3D polymerase activity and virus**
356 **replication.**

357 Among the two SUMOylation sites in 3D, K159 is a highly conserved active site
358 residue in RdRp motif F and within hydrogen-bonding distances to the edge of the
359 nascent base pair of the RdRp elongation complex, while the 150-152 site is on the
360 surface of 3D and does not directly participate in either RNA binding, NTP entry, and
361 catalysis (Fig. 4B) (56). With an aim to assess the relevance of both SUMOylation
362 sites to the polymerase function, we conducted primer-dependent polymerase assays
363 (58, 64) for wild-type (WT) 3D and the K159R, K159A, and L150A/D151A mutants.
364 With the usage of the T33/P10 RNA construct and GTP/ATP as the only substrates,
365 the 10-nucleotide primer (P10) was expected to elongate by four nucleotides,
366 producing a 14-nucleotide product (58). For the WT enzyme, the majority of the

primer was converted to the product within 60-min incubation time (Fig. 4C, 4D). The K159R mutant enzyme exhibited similar high conversion yield, while the K159A and L150A/D151A mutants had obviously lower yield with only 40% of primer converted judged by band intensity (Fig. 4C, 4D). These data in general suggest that both SUMOylation sites in 3D may modulate EV71 polymerase activity, despite their differences in structural properties based on available crystallographic data (56, 64).

To assess the effect of 3D SUMOylation sites on EV71 replication, we constructed the IF-K159R and IF-K159R/150-152 SIM recombinant viruses. Unfortunately, both recombinant viruses were unable to be rescued. However, transfection of WT 3D protein and K159R recombinant RNA resulted in the rescue of wild-type virus. A L150A/D151A mutant was constructed to map the critical region. Since the L150A/D151A mutant can largely decrease the SUMO-1 modification (Fig. 3C), we also tested the IF-L150A/D151A recombinant virus. As shown in Figure 4E the growth curve of this recombinant virus was significant lower than that of wild-type virus. Therefore, the lower titer of IF-L150A/D151A was likely due to the decreased enzyme activity or/and lack of SUMOylation.

3D protein is SUMOylated *in vitro*

SUMOylation is a process of enzyme-catalyzed reactions. Two-component vector systems carrying SAE1, SAE2, Ubc9, SUMO-1 and the target protein in *E.coli* were used to generate SUMOylated proteins *in vitro* (55). In the present study, we used the method by transforming *E. coli* with pSUMO-1-Strep and pGEX-6p-3D to produce

388 SUMOylated proteins (Fig. 5A). SUMO-1 modified proteins were confirmed by
389 SDS-PAGE and immunoblot. Under IPTG induction, the results of Coomassie blue
390 staining and immunoblot showed that BL21 (pSUMO-1-Strep and pGEX-6p-3D)
391 strains not only expressed 3D-GST but also 3D-GST-SUMO-1s (Fig. 5B, Lanes 3 and
392 4). By contrast, BL21 (pGEX-6p-3D) only produced 3D-GST (Fig. 5B, Lane 1 and 6).
393 After induction, the cell lysates of BL21 (pSUMO-1-Strep and pGEX-6p-3D) strains
394 were subjected to subsequent GST and Strep affinity chromatography. The collected
395 protein samples were resolved by SDS-PAGE and visualized by Coomassie blue
396 staining (Fig. 5C). SUMOylated 3D was verified by immunoblotting with the anti-3D
397 or anti-SUMO-1 antibody (Fig. 5D). These results indicate that EV71 3D can be
398 modified by SUMO-1 *in vitro*.

399 **3D is ubiquitinated in a SUMOylation-dependent manner**

400 The ubiquitin–proteasome system (UPS) is required for the effective replication of
401 both coxsackievirus B3 (CVB3) (65) and EV71 (66). Since SUMOylation can
402 interplay with ubiquitination in many viral proteins, we determined whether EV71 3D
403 is ubiquitinated. Flag-3D and K159R/150-152 SIM were co-expressed with HA-Ub in
404 293T cells for ubiquitination assay (Fig. 6A). The cell lysates were subjected to
405 immunoprecipitation with the anti-Flag antibody. Immunoblot by the anti-HA
406 antibody showed that 3D could be poly-ubiquitinated (polyUb), whereas the mutant
407 K159R/150-152 SIM almost lost this modification.

408 The above experiments implied that ubiquitination and SUMOylation of 3D may

409 share the same lysine residues and 3D ubiquitination was SUMOylation related. To
410 determine the association between the two modifications, SENP-1 and lysine-less
411 ubiquitin Ub (KO) were introduced into 3D SUMOylation and ubiquitination
412 experiments. Ub (KO) terminates ubiquitin chain, and it was created by replacing all
413 lysines with arginines. Ub (KO) had dose-dependent effect on the ubiquitin system
414 when Ub (KO) was overexpressed to compete with the endogenous ubiquitin (67). In
415 our study, 3D ubiquitination was increased when Ub was co-expressed with SUMO
416 and Ubc9 (Fig. 6B). Co-expression of SENP-1 decreased both 3D SUMOylation and
417 ubiquitination, which was in accordance with the results of the mutant
418 K159R/150-152SIM. The co-expression of Ub (KO) resulted in the reduction of 3D
419 ubiquitination, but it hardly had any effect on 3D.

420 We further investigated whether 3D ubiquitination level could be altered according to
421 the gradient expression of SENP-1 or SUMO-1 in 293T cells. The ubiquitination level
422 was enhanced when the SUMOylation of 3D was increased (Fig. 6C). On the contrary,
423 the increased expression of SENP-1 gradually reduced the amount of ubiquitin
424 conjugated on 3D (Fig. 6D). Taken together, these data imply that the two
425 modifications sequentially occur, with ubiquitination being highly
426 SUMOylation-dependent.

427 **SUMO-1 modification enhances the stability of 3D**

428 Normally, the polyUbs are primarily linked through K48 or K63 to play diverse roles
429 in regulating cellular activities, which account for 52 % and 38 % of all ubiquitination

events, respectively (68). K48-linked ubiquitination chains are involved in proteasomal degradation, whereas K63-linked ubiquitination is a docking site for mediating protein–protein interactions or conformational changes (69). To explore which kind of polyUb 3D is linked and whether 3D is degraded, we transfected 3D and K159R/150-152 SIM together with HA-K48-Ub or HA-K63-Ub to perform the ubiquitination assay. 3D was specifically modified by K63-linked ubiquitin, whereas the K159R/150-152 SIM significantly reduced the conjugation (Fig. 7A). Noticeably, no degradation of 3D was observed in the assay (Fig. 7A).

CHX chase experiments were then carried out to determine the stability difference between 3D and K159R/150-152 SIM. 3D exhibited longer half-life than K159R/150-152 SIM, and the MG132 treatment attenuated K159R/150-152 SIM degradation (Fig. 7B, 7C). These results imply that SUMOylation-related K63-linked ubiquitination may stabilize 3D.

Elevated SUMO-1 expression level increases EV71 replication

To analyze the effects of SUMO-1 overexpression on virus production, SUMO-1 and Ubc9 were transiently transfected into 293T cells. The cells were subsequently infected with EV71 for 18 h. The SUMOylation and ubiquitination levels of viral 3D increased in the condition of SUMO-1 overexpression (Fig. 8A). 3CD protein was detected by anti-3C antibody. These results implied that though IP by an anti-3D antibody could co-immunoprecipitated 3D, 3CD, and 3BCD, while data from the anti-SUMO-1 antibody indicated that 3D was indeed modified by SUMO-1. The

451 expression of viral 3D and VP1 were increased when SUMOylation level was
452 enhanced (Fig. 8B). The titer of EV71 produced from SUMOylation-increased 293T
453 cells was higher than that from 293T transfected with the empty vector (Fig. 8C).
454 Collectively, these results indicated that elevation of the global cell SUMOylation
455 increased both SUMOylation and ubiquitination level of 3D, which augmented 3D
456 expression and consequently enhanced viral replication.

457 **Discussion**

458 A number of viral proteins have been reported to be modified by SUMO moieties (22,
459 62). However, the knowledge concerning SUMOylation in enteroviruses is limited.
460 Only EV71 3C protease is SUMOylated, while coxsackievirus B5 is involved in the
461 host cell SUMOylation system in the *Picornaviridae* family (38, 62, 70). Current
462 understanding of viral polymerases SUMOylation is limited to RdRp of *Turnip*
463 *Mosaic Virus* (71), DNA polymerase subunit UL44 of HCMV (25), nonstructural
464 protein 5 (NS5) of dengue virus (72), and polymerase basic protein PB1 of influenza
465 virus (30). In the currently study, we reveal that the 3D protein of EV71, a
466 RNA-dependent RNA polymerase, is SUMOylated. We found that EV71 3D
467 polymerase is modified by SUMO-1 both *in vivo* and *in vitro* and that 3D is stabilized
468 by SUMOylation-related ubiquitination. K159 and L150/D151/L152 are responsible
469 for 3D SUMOylation. Mutations of SUMOylation sites impaired 3D polymerase
470 activity and virus replication. Moreover, elevated SUMOylation level during EV71
471 infection resulted in promoted 3D stability which enhanced viral replication. We

propose that SUMOlyation at specific 3D sites help maintain the cellular level of 3D protein and the corresponding de-SUMOlyation may be necessary for 3D to resume its polymerase activity. The 3D polymerase function may be only required when it is responsible for the RNA genome replication which is SUMOylation free. These findings implicate that EV71 exploits host proteins for its effective infection and that the SUMO system is likely to be a putative antiviral target.

Online prediction indicated that 3D is bearing both covalent and non-covalent sites for SUMOylation. According to the predictions, K159, K427, and K376 are on the top three of the list following the pattern of ψ-K-X-D/E motif (http://www.abgent.com/sumoplot.html), while V263/S264/L265 is the putative SUMO-interacting motif (SIM) (63). In our study, K159 and L150/D151/L152 as SIM are proven to be the SUMOylation sites, while K159 follows the classic consensus motif of ψ-K-X-D/E and is the major site for SUMO-1 modification (Fig. 3A). However, although L150/D151/L152 is not within the predicted SUMOylation sites of 3D, they have been proven to be a SIM in our study. Additionally, the inverted consensus motif E/D-X-K-ψ worked for EV71 3C but not for 3D (38). In fact, the bioinformatic prediction software is based on the calculation of the reported SUMOylation site, and some unknown limitations may exist. Therefore, there may be SUMOylation sites that cannot be predicted by bioinformatic software. For instance, mutation of the predicted SUMOylation sites in human Cytomegalovirus DNA polymerase processivity factor UL44 hardly attenuates the modification (25). Herein, our findings of L150/D151/L152 as SIM site may expand the data pool for developing

494 higher confidences algorithm.

495 Normally, the interplay between SUMOylation and ubiquitination often involves the
496 stability of the target protein. (73). SUMOylation and K48-linked ubiquitination of
497 IRF3 share the same lysine residues and the two processes are competitive, indicating
498 that SUMOylation of IRF3 stabilizes the protein by antagonizing ubiquitination (51).
499 SUMOylation of EV71 3C protease shares the same K52 with its ubiquitination, and
500 consequently enhances ubiquitination which leads to the degradation of 3C (38).
501 Other study showed how the two PTMs cooperatively stabilized target proteins in
502 various ways. For instance, the E3 protein of vaccinia virus is modified by both
503 SUMOylation and ubiquitination. Wild-type E3 exhibited longer half-life than its SIM
504 mutant. It was speculated that the different stabilities observed between the wild-type
505 E3 and the SIM-mutant were due to the longer ubiquitin chains conjugated on
506 SIM-mutant (74). SUMOylation stabilizes dengue virus NS5 from proteasome
507 degradation which supports virus replication (72). SUMO-1 stabilizes phosducin, and
508 the authors inferred that SUMO moieties conjugated on phosducin may mask the
509 region recognized by ubiquitin-proteasome pathway (75). Following gradient
510 overexpression of SUMO-1 and Ubc9 or SENP-1 with 3D, the results showed that the
511 level of ubiquitination was highly dependent on SUMOylation. Moreover, when Ub
512 was substituted with Ub (KO), 3D ubiquitination was reduced, although it hardly had
513 any effect on 3D SUMOylation. Taken together, these results implied that
514 poly-SUMO chain likely act as a signal for 3D ubiquitination. In such case, ubiquitin
515 might be hybridized with poly-SUMO chains or be conjugated on the exposed internal

516 residues of 3D due to the conformational change induced by SUMOylation. The
517 importance of UPS during replication of both coxsackievirus B3 (CVB3) and EV71
518 may rely on 3D SUMOylation (65, 66). We found that the degradation of 3D by
519 K63-linked ubiquitination was not observed and that wild-type 3D showed longer
520 half-life than the SUMOylation-deficient mutant K159R/150-152 SIM. The
521 K63-linked poly-ubiquitination generally has non-proteolytic cellular functions,
522 including DNA damage repair, stress responses, and inflammatory pathways (76).
523 Taken together, SUMO-moieties conjugated on 3D act as a signal for K63-linked
524 ubiquitination which cooperatively stabilizes 3D.

525 K159 is within RdRp catalytic motif F and is highly conserved in positive-strand
526 RNA viruses (77). Structurally, this residue is located in the polymerase active site
527 and within hydrogen-bonding distance to the nascent base pair (Fig. 4B) (56, 64, 78).
528 Therefore, it is not surprising that the K159A mutation reduces *in vitro* polymerase
529 activity (Fig. 4C, 4D). The K159R mutation, however, retained WT level polymerase
530 activity in our test but the corresponding recombinant virus was not viable. Despite
531 being an amino acid with a basic side chain, the arginine may be not ideal to replace
532 the native lysine at this critical position. Due to its critical roles in polymerase
533 catalysis, we tend to believe that the defects in polymerase catalysis (although not
534 clarified in our *in vitro* assays) rather than the loss of SUMOlyation property accounts
535 for the inviability of the recombinant virus IF-K159R. Compared to K159, the
536 150-152 SIM is moderately conserved only in enteroviruses and is located near the
537 polymerase surface (Fig. 4B), and therefore it is unlikely to play major roles in

538 polymerase catalysis. Although the *in vitro* enzyme activity of L150A/D151A was
539 lower than that of 3D, the recombinant virus IF-L150A/D151A was successfully
540 rescued. The fact that the titer of IF-L150A/D151A recombinant virus was lower than
541 that of the WT EV71 was likely due to the reduced enzyme activity, or/and the
542 impairment of SUMOylation. To reinforce the deduction, we adopted a method by
543 overexpressing SUMO-1 to determine how SUMOylation system could affect EV71
544 infection. EV71 infection in SUMOylation elevated 293T cells showed that more
545 SUMO-1 led to higher ubiquitination of 3D which increased virus production
546 compared with the cells transfected with empty vector. It is reported that EV71 3C
547 K52R SUMOylation deficient virus showed elevated virus titer compared to wild-type
548 virus (38). The increased titer of EV71 from SUMO-1 overexpressed cells was likely
549 due to higher SUMOylation and ubiquitination on 3D, which may eventually stabilize
550 3D and the augmented polymerases promoted EV71 replication. Other than the results
551 from EV71 3C SUMOylation, the increased gobal SUMOylation level is beneficial
552 for EV71 replication. Although 3C and 3D SUMOylation have opposite consequences
553 during EV71 replication, the influence of 3D SUMOylation is greater than that of 3C.
554 As a polymerase, any modification on 3D may affect virus replication, and in the case
555 of SUMOylation, the impact is favorable for the virus replication. These results
556 suggested that EV71 may exploit the SUMOylation-related ubiquitination to facilitate
557 its replication by protecting the 3D polymerase.

558 Timely turning on and off of SUMO signaling on viral proteins is important for virus
559 replication (32). Given that 3D is a RdRp, the maintenance of an appropriate level of

RdRp in infected cells is crucial for viral growth, as lower amount of RdRp may be beneficial for the virus to escape host immune systems (79, 80). It is worthy to note that the SUMOylation of 3D and the RNA synthesis by 3D may well be two processes with relative independence. Based on the chemical nature of polymerase catalysis and the SUMOlyation process, at least the covalent SUMOlyation at K159 is not compatible with polymerase catalysis. We propose that SUMOlyation at specific 3D sites help maintain the cellular level of 3D protein and the corresponding de-SUMOlyation may be necessary for 3D to resume its polymerase activity, in particular for the critical site of K159. In summary, our findings showed that ubiquitination of EV71 3D is SUMOylation-dependent. EV71 may exploit the crosstalk of SUMOylation and ubiquitination to stabilize the 3D polymerase and enhance viral replication, which may provide new insights on antivirus by targeting the SUMOylation of EV71 3D.

Funding information

This work was supported by National Natural Science Foundation of China (Grant 31 300152 and Grant 81371811). The funders had no role in study design, data collection and interpretation, or the decision to submit the work for publication.

Acknowledgments

We thank Hsiu-Ming Shih (Institute of Biomedical Sciences, Academia Sinica, Taiwan, Republic of China) for his helpful suggestions on conducting the experiments.

And we thank Hong Tang (Wuhan Institute of Virology, Chinese Academy of Sciences, Wuhan, China) for providing plasmids pcDEF-HA-SUMO-1, pcDEF-Myc-Ubc9, and pcDEF-Flag-SUMO-2. We thank Yanyi Wang (Wuhan Institute of Virology, Chinese Academy of Sciences, Wuhan, China) for providing plasmid pRK-Flag-SUMO-2. We thank Huimin Yan (Wuhan Institute of Virology, Chinese Academy of Sciences, Wuhan, China) for providing anti-3D antibody. And we thank Minetaro Arita (National Institute of Infectious Diseases, Tokyo, Japan) for providing the infectious clone of EV71.

Reference

1. **Meulmeester E, Melchior F.** 2008. Cell biology: SUMO. Nature **452:**709-711.
2. **Bayer P, Arndt A, Metzger S, Mahajan R, Melchior F, Jaenicke R, Becker J.** 1998. Structure determination of the small ubiquitin-related modifier SUMO-1. J Mol Biol **280:**275-286.
3. **Tatham MH, Jaffray E, Vaughan OA, Desterro JMP, Botting CH, Naismith JH, Hay RT.** 2001. Polymeric chains of SUMO-2 and SUMO-3 are conjugated to protein substrates by SAE1/SAE2 and Ubc9. Journal of Biological Chemistry **276:**35368-35374.
4. **Bylebyl GR, Belichenko I, Johnson ES.** 2003. The SUMO isopeptidase Ulp2 prevents accumulation of SUMO chains in yeast. The Journal of biological chemistry **278:**44113-44120.
5. **Matic I, van Hagen M, Schimmel J, Macek B, Ogg SC, Tatham MH, Hay RT, Lamond AI, Mann M, Vertegaal ACO.** 2008. In vivo identification of human small ubiquitin-like modifier polymerization sites by high accuracy mass spectrometry and an in vitro to in vivo strategy. Molecular & Cellular Proteomics **7:**132-144.

6. **Wang YG, Dasso M.** 2009. SUMOylation and deSUMOylation at a glance. J Cell Sci **122:**4249-4252.

7. **Everett RD, Boutell C, Hale BG.** 2013. Interplay between viruses and host sumoylation pathways. Nat Rev Microbiol **11:**400-411.

8. **Hay RT.** 2007. SUMO-specific proteases: a twist in the tail. Trends Cell Biol **17:**370-376.

9. **Johnson ES, Blobel G.** 1997. Ubc9p is the conjugating enzyme for the ubiquitin-like protein Smt3p. Journal of Biological Chemistry **272:**26799-26802.

10. **Hayashi T, Seki M, Maeda D, Wang WS, Kawabe Y, Seki T, Saitoh H, Fukagawa T, Yagi H, Enomoto T.** 2002. Ubc9 is essential for viability of higher eukaryotic cells. Exp Cell Res **280:**212-221.

11. **Bernier-Villamor V, Sampson DA, Matunis MJ, Lima CD.** 2002. Structural basis for E2-mediated SUMO conjugation revealed by a complex between ubiquitin-conjugating enzyme Ubc9 and RanGAP1. Cell **108:**345-356.

12. **Gareau JR, Lima CD.** 2010. The SUMO pathway: emerging mechanisms that shape specificity, conjugation and recognition. Nat Rev Mol Cell Bio **11:**861-871.

13. **Hay RT.** 2005. SUMO: A history of modification. Mol Cell **18:**1-12.

14. **Merrill JC, Melhuish TA, Kagey MH, Yang SH, Sharrocks AD, Wotton D.** 2010. A role for non-covalent SUMO interaction motifs in Pc2/CBX4 E3 activity. PloS one **5:**e8794.

15. **Song J, Durrin LK, Wilkinson TA, Krontiris TG, Chen Y.** 2004. Identification of a SUMO-Binding motif that recognizes SUMO modified proteins. Mol Biol Cell **15:**119a-119a.

16. **Song J, Zhang ZM, Hu WD, Chen Y.** 2005. Small ubiquitin-like modifier (SUMO) recognition of a SUMO binding motif - A reversal of the bound orientation. Journal of Biological Chemistry **280:**40122-40129.

17. **Sun HY, Hunter T.** 2012. Poly-Small Ubiquitin-like Modifier (PolySUMO)-binding Proteins Identified through a String Search. Journal of Biological Chemistry **287:**42071-42083.

18. **Kravtsova-Ivantsiv Y, Ciechanover A.** 2012. Non-canonical ubiquitin-based signals for proteasomal degradation. J Cell Sci **125:**539-548.

19. **Guzzo CM, Matunis MJ.** 2013. Expanding SUMO and ubiquitin-mediated signaling through hybrid SUMO-ubiquitin chains and their receptors. Cell cycle **12:**1015-1017.

20. **Praefcke GJK, Hofmann K, Dohmen J.** 2012. SUMO playing tag with ubiquitin. Trends

Biochem Sci **37:**23-31.

21. **Denuc A, Marfany G.** 2010. SUMO and ubiquitin paths converge. Biochemical Society transactions **38:**34-39.

22. **Mattoscio D, Segre CV, Chiocca S.** 2013. Viral manipulation of cellular protein conjugation pathways: The SUMO lesson. World journal of virology **2:**79-90.

23. **Nevels M, Brune W, Shenk T.** 2004. SUMOylation of the human cytomegalovirus 72-kilodalton IE1 protein facilitates expression of the 86-kilodalton IE2 protein and promotes viral replication. Journal of virology **78:**7803-7812.

24. **Hofmann H, Floss S, Stamminger T.** 2000. Covalent modification of the transactivator protein IE2-p86 of human cytomegalovirus by conjugation to the ubiquitin-homologous proteins SUMO-1 and hSMT3b. Journal of virology **74:**2510-2524.

25. **Sinigalia E, Alvisi G, Segre CV, Mercorelli B, Muratore G, Winkler M, Hsiao HH, Urlaub H, Ripalti A, Chiocca S, Palu G, Loregian A.** 2012. The Human Cytomegalovirus DNA Polymerase Processivity Factor UL44 Is Modified by SUMO in a DNA-Dependent Manner. PloS one **7**.

26. **Kim ET, Kim YE, Huh YH, Ahn JH.** 2010. Role of Noncovalent SUMO Binding by the Human Cytomegalovirus IE2 Transactivator in Lytic Growth. Journal of virology **84:**8111-8123.

27. **Pal S, Santos A, Rosas JM, Ortiz-Guzman J, Rosas-Acosta G.** 2011. Influenza A virus interacts extensively with the cellular SUMOylation system during infection. Virus research **158:**12-27.

28. **Xu K, Klenk C, Liu B, Keiner B, Cheng J, Zheng BJ, Li L, Han Q, Wang C, Li T, Chen Z, Shu Y, Liu J, Klenk HD, Sun B.** 2011. Modification of nonstructural protein 1 of influenza A virus by SUMO1. Journal of virology **85:**1086-1098.

29. **Wu CY, Jeng KS, Lai MM.** 2011. The SUMOylation of matrix protein M1 modulates the assembly and morphogenesis of influenza A virus. Journal of virology **85:**6618-6628.

30. **Han QL, Chang C, Li L, Klenk C, Cheng JK, Chen YX, Xia NS, Shu YL, Chen Z, Gabriel G, Sun B, Xu K.** 2014. Sumoylation of Influenza A Virus Nucleoprotein Is Essential for Intracellular Trafficking and Virus Growth. Journal of virology **88:**9379-9390.

31. **Izumiya Y, Ellison TJ, Yeh ET, Jung JU, Luciw PA, Kung HJ.** 2005. Kaposi's

sarcoma-associated herpesvirus K-bZIP represses gene transcription via SUMO modification. Journal of virology **79:**9912-9925.

32. **Izumiya Y, Kobayashi K, Kim KY, Pochampalli M, Izumiya C, Shevchenko B, Wang DH, Huerta SB, Martinez A, Campbell M, Kung HJ.** 2013. Kaposi's sarcoma-associated herpesvirus K-Rta exhibits SUMO-targeting ubiquitin ligase (STUbL) like activity and is essential for viral reactivation. PLoS pathogens **9:**e1003506.

33. **Marcos-Villar L, Campagna M, Lopitz-Otsoa F, Gallego P, Gonzalez-Santamaria J, Gonzalez D, Rodriguez MS, Rivas C.** 2011. Covalent modification by SUMO is required for efficient disruption of PML oncogenic domains by Kaposi's sarcoma-associated herpesvirus latent protein LANA2. J Gen Virol **92:**188-194.

34. **Gurer C, Berthoux L, Luban J.** 2005. Covalent modification of human immunodeficiency virus type 1 p6 by SUMO-1. Journal of virology **79:**910-917.

35. **Zamborlini A, Coiffic A, Beauclair G, Delelis O, Paris J, Koh Y, Magne F, Giron ML, Tobaly-Tapiero J, Deprez E, Emiliani S, Engelman A, de The H, Saib A.** 2011. Impairment of human immunodeficiency virus type-1 integrase SUMOylation correlates with an early replication defect. The Journal of biological chemistry **286:**21013-21022.

36. **AbuBakar S, Chee HY, Al-Kobaisi MF, Xiaoshan J, Chua KB, Lam SK.** 1999. Identification of enterovirus 71 isolates from an outbreak of hand, foot and mouth disease (HFMD) with fatal cases of encephalomyelitis in Malaysia. Virus research **61:**1-9.

37. **McMinn PC.** 2002. An overview of the evolution of enterovirus 71 and its clinical and public health significance. Fems Microbiol Rev **26:**91-107.

38. **Chen SC, Chang LY, Wang YW, Chen YC, Weng KF, Shih SR, Shih HM.** 2011. Sumoylation-promoted enterovirus 71 3C degradation correlates with a reduction in viral replication and cell apoptosis. The Journal of biological chemistry **286:**31373-31384.

39. **Zheng Z, Ke X, Wang M, He S, Li Q, Zheng C, Zhang Z, Liu Y, Wang H.** 2013. Human microRNA hsa-miR-296-5p suppresses enterovirus 71 replication by targeting the viral genome. Journal of virology **87:**5645-5656.

40. **Pizzi M.** 1950. Sampling variation of the fifty percent end-point, determined by the Reed-Muench (Behrens) method. Human biology **22:**151-190.

41. **Gong Y, Trowbridge R, Macnaughton TB, Westaway EG, Shannon AD, Gowans EJ.**

1996. Characterization of RNA synthesis during a one-step growth curve and of the replication mechanism of bovine viral diarrhoea virus. J Gen Virol **77 (Pt 11):**2729-2736.

42. **Arita M, Shimizu H, Nagata N, Ami Y, Suzaki Y, Sata T, Iwasaki T, Miyamura T.** 2005. Temperature-sensitive mutants of enterovirus 71 show attenuation in cynomolgus monkeys. J Gen Virol **86:**1391-1401.

43. **Wang G, Cao RY, Chen R, Mo L, Han JF, Wang X, Xu X, Jiang T, Deng YQ, Lyu K, Zhu SY, Qin ED, Tang R, Qin CF.** 2013. Rational design of thermostable vaccines by engineered peptide-induced virus self-biomineralization under physiological conditions. Proceedings of the National Academy of Sciences of the United States of America **110:**7619-7624.

44. **Chen Z, Sahashi Y, Matsuo K, Asanuma H, Takahashi H, Iwasaki T, Suzuki Y, Aizawa C, Kurata T, Tamura S.** 1998. Comparison of the ability of viral protein-expressing plasmid DNAs to protect against influenza. Vaccine **16:**1544-1549.

45. **Zheng Z, Li H, Zhang Z, Meng J, Mao D, Bai B, Lu B, Mao P, Hu Q, Wang H.** 2011. Enterovirus 71 2C protein inhibits TNF-alpha-mediated activation of NF-kappaB by suppressing IkappaB kinase beta phosphorylation. Journal of immunology **187:**2202-2212.

46. **Terui Y, Saad N, Jia S, McKeon F, Yuan J.** 2004. Dual role of sumoylation in the nuclear localization and transcriptional activation of NFAT1. The Journal of biological chemistry **279:**28257-28265.

47. **Kamitani T, Nguyen HP, Kito K, Fukuda-Kamitani T, Yeh ET.** 1998. Covalent modification of PML by the sentrin family of ubiquitin-like proteins. The Journal of biological chemistry **273:**3117-3120.

48. **Cheng J, Kang XL, Zhang S, Yeh ETH.** 2007. SUMO-Specific protease 1 is essential for stabilization of HIF1 alpha during hypoxia. Cell **131:**584-595.

49. **Yasugi T, Howley PM.** 1996. Identification of the structural and functional human homolog of the yeast ubiquitin conjugating enzyme UBC9. Nucleic acids research **24:**2005-2010.

50. **Mi Z, Fu J, Xiong Y, Tang H.** 2010. SUMOylation of RIG-I positively regulates the type I interferon signaling. Protein & cell **1:**275-283.

51. **Ran Y, Liu TT, Zhou Q, Li S, Mao AP, Li Y, Liu LJ, Cheng JK, Shu HB.** 2011. SENP2 negatively regulates cellular antiviral response by deSUMOylating IRF3 and conditioning it for ubiquitination and degradation. Journal of molecular cell biology **3:**283-292.

724 52. **Luo H, Zhang Z, Zheng Z, Ke X, Zhang X, Li Q, Liu Y, Bai B, Mao P, Hu Q, Wang H.**
725 2013. Human bocavirus VP2 upregulates IFN-beta pathway by inhibiting ring finger protein
726 125-mediated ubiquitination of retinoic acid-inducible gene-I. Journal of immunology
727 **191:**660-669.
728 53. **Gong P, Campagnola G, Peersen OB.** 2009. A quantitative stopped-flow fluorescence assay
729 for measuring polymerase elongation rates. Analytical biochemistry **391:**45-55.
730 54. **Gohara DW, Ha CS, Kumar S, Ghosh B, Arnold JJ, Wisniewski TJ, Cameron CE.** 1999.
731 Production of "authentic" poliovirus RNA-dependent RNA polymerase (3D(pol)) by
732 ubiquitin-protease-mediated cleavage in Escherichia coli. Protein expression and purification
733 **17:**128-138.
734 55. **Weber AR, Schuermann D, Schar P.** 2014. Versatile recombinant SUMOylation system for
735 the production of SUMO-modified protein. PloS one **9:**e102157.
736 56. **Shu B, Gong P.** 2016. Structural basis of viral RNA-dependent RNA polymerase catalysis and
737 translocation. Proceedings of the National Academy of Sciences of the United States of
738 America **113:**E4005-4014.
739 57. **Batey RT, Kieft JS.** 2007. Improved native affinity purification of RNA. Rna **13:**1384-1389.
740 58. **Wu J, Lu G, Zhang B, Gong P.** 2015. Perturbation in the conserved
741 methyltransferase-polymerase interface of flavivirus NS5 differentially affects polymerase
742 initiation and elongation. Journal of virology **89:**249-261.
743 59. **Campagnola G, Weygandt M, Scoggin K, Peersen O.** 2008. Crystal structure of
744 coxsackievirus B3 3Dpol highlights the functional importance of residue 5 in picornavirus
745 polymerases. Journal of virology **82:**9458-9464.
746 60. **Kao S, Wang, W., Chen, C., Chang, Y., Wu, Y., Wang, Y., Wang, S., Nesvizhskii, A. I.,**
747 **Chen, Y., Hong, T. and Yang, P. .** 2015. Analysis of Protein Stability by the Cycloheximide
748 Chase Assay. Bio-protocol **5:**e1374.
749 61. **Saitoh H, Hinchey J.** 2000. Functional heterogeneity of small ubiquitin-related protein
750 modifiers SUMO-1 versus SUMO-2/3. The Journal of biological chemistry **275:**6252-6258.
751 62. **Wimmer P, Schreiner S, Dobner T.** 2012. Human Pathogens and the Host Cell
752 SUMOylation System. Journal of virology **86:**642-654.
753 63. **Zhao Q, Xie Y, Zheng Y, Jiang S, Liu W, Mu W, Liu Z, Zhao Y, Xue Y, Ren J.** 2014.

GPS-SUMO: a tool for the prediction of sumoylation sites and SUMO-interaction motifs. Nucleic acids research **42:**W325-330.

64. **Gong P, Peersen OB.** 2010. Structural basis for active site closure by the poliovirus RNA-dependent RNA polymerase. Proceedings of the National Academy of Sciences of the United States of America **107:**22505-22510.

65. **Si XN, Gao G, Wong J, Wang YH, Zhang JC, Luo HL.** 2008. Ubiquitination Is Required for Effective Replication of Coxsackievirus B3. PloS one **3**.

66. **Lin L, Qin Y, Wu H, Chen Y, Wu S, Si X, Wang H, Wang T, Zhong X, Zhai X, Tong L, Pan B, Zhang F, Zhong Z, Wang Y, Zhao W.** 2015. Pyrrolidine dithiocarbamate inhibits enterovirus 71 replication by down-regulating ubiquitin-proteasome system. Virus research **195:**207-216.

67. **Bloom J, Pagano M.** 2005. Experimental tests to definitively determine ubiquitylation of a substrate. Methods in enzymology **399:**249-266.

68. **Dammer EB, Na CH, Xu P, Seyfried NT, Duong DM, Cheng D, Gearing M, Rees H, Lah JJ, Levey AI, Rush J, Peng J.** 2011. Polyubiquitin linkage profiles in three models of proteolytic stress suggest the etiology of Alzheimer disease. The Journal of biological chemistry **286:**10457-10465.

69. **Mallette FA, Richard S.** 2012. K48-linked ubiquitination and protein degradation regulate 53BP1 recruitment at DNA damage sites. Cell Res **22:**1221-1223.

70. **Gomes R, Guerra-Sa R, Arruda E.** 2010. Coxsackievirus B5 induced apoptosis of HeLa cells: effects on p53 and SUMO. Virology **396:**256-263.

71. **Xiong RY, Wang AM.** 2013. SCE1, the SUMO-Conjugating Enzyme in Plants That Interacts with NIb, the RNA-Dependent RNA Polymerase of Turnip Mosaic Virus, Is Required for Viral Infection. Journal of virology **87:**4704-4715.

72. **Su CI, Tseng CH, Yu CY, Lai MM.** 2016. SUMO Modification Stabilizes Dengue Virus Nonstructural Protein 5 To Support Virus Replication. Journal of virology **90:**4308-4319.

73. **Maria Miteva KK, Kay Hofmann,Gerrit J.K. Praefcke and R. Jürgen Dohmen*.** 2010. SUMOylation as a signal for polyubiquitylation and proteasomal degradation, p. 195-215. *In* Groettrup M (ed.), Conjugation and Deconjugation of Ubiquitin Family Modifiers. Landes Bioscience and Springer Science+Business Media.

74. **Gonzalez-Santamaria J, Campagna M, Garcia MA, Marcos-Villar L, Gonzalez D, Gallego P, Lopitz-Otsoa F, Guerra S, Rodriguez MS, Esteban M, Rivas C.** 2011. Regulation of Vaccinia Virus E3 Protein by Small Ubiquitin-Like Modifier Proteins. Journal of virology **85:**12890-12900.

75. **Klenk C, Humrich J, Quitterer U, Lohse MJ.** 2006. SUMO-1 controls the protein stability and the biological function of phosducin. Journal of Biological Chemistry **281:**8357-8364.

76. **Zhang L, Xu M, Scotti E, Chen ZJJ, Tontonoz P.** 2013. Both K63 and K48 ubiquitin linkages signal lysosomal degradation of the LDL receptor. J Lipid Res **54:**1410-1420.

77. **Bruenn JA.** 2003. A structural and primary sequence comparison of the viral RNA-dependent RNA polymerases. Nucleic acids research **31:**1821-1829.

78. **Wu Y, Lou Z, Miao Y, Yu Y, Dong H, Peng W, Bartlam M, Li X, Rao Z.** 2010. Structures of EV71 RNA-dependent RNA polymerase in complex with substrate and analogue provide a drug target against the hand-foot-and-mouth disease pandemic in China. Protein & cell **1:**491-500.

79. **Kerkvliet J, Papke L, Rodriguez M.** 2011. Antiviral effects of a transgenic RNA-dependent RNA polymerase. Journal of virology **85:**621-625.

80. **Choi AG, Wong J, Marchant D, Luo H.** 2013. The ubiquitin-proteasome system in positive-strand RNA virus infection. Reviews in medical virology **23:**85-96.

Figure Legends

Figure 1. EV71 3D is SUMOylated during infection. 1×10^7 RD cells were infected with EV71 virus (MOI = 10) and harvested at 8 h post-infection before immunoprecipitation with an anti-3D antibody. Immunoprecipitation (IP) and immunoblot (IB) analyses were performed with the indicated antibodies in the presence of NEM. (A) Immunoblot detected by anti-SUMO-1, anti-Ub, anti-3C and anti-3D antibodies during EV71 infection after immunoprecipitation by the anti-3D antibody. (B) Immunoblot analysis of the cell lysis during infection. Anti-VP1, anti-3D and anti-beta actin antibodies were used to detect the expression of VP1, 3D and beta-actin during infection. Lysis of RD cells without infection

was set as MOCK control. SUMO-1 modified 3D, ubiquitin modified 3D, and 3CD are depicted by asterisks, brackets, and arrows, respectively.

Figure 2. EV71 3D is modified by SUMO-1 and 3. (A) SUMOylation of EV71 3D in the presence of NEM. 293T cells were transfected with Flag-3D, Myc-Ubc9, and HA-SUMO-1. Cells were lysed with or without the addition of NEM, which was added to a final concentration of 20 mM prepared in ethanol. Immunoprecipitation and immunoblot analysis were performed with the indicated antibodies for SUMOylation assay. (B) DeSUMOylation of 3D by SENP-1. 293T cells were transfected with Flag-3D, Myc-Ubc9, HA-SUMO-1, and V5-SENP-1. Immunoprecipitation and immunoblot analysis were performed with the indicated antibodies in the presence of NEM. (C) 3D interacted with Ubc9. 293T cells were transfected with Flag-3D, Myc-Ubc9, or empty vector. Co-immunoprecipitation was performed with anti-flag or control mouse IgG; immunoblots were probed with the corresponding antibodies. (D) 3D was modified by SUMO-1 and 3. Flag-3D, Myc-Ubc9, HA-SUMO-1, HA-SUMO-2, and HA-SUMO-3 were overexpressed in 293T cells. Immunoprecipitation and immunoblot analysis were performed with the indicated antibodies in the presence of NEM. Molecular size markers are shown in kilodaltons (kDa). SUMO-1 modified Flag-3Ds are depicted by brackets.

Figure 3. Identification of Lys159 and Leu150/Asp151/Leu152 as major SUMOylation sites. (A) SUMOylation assay of 3D and its single site mutants based on the canonical consensus motif. The lysine residue at 159, 323, 376, and 427 were replaced by arginine to create K159R, K323R, K376R and K427R. (B) SUMOylation assay of 3D and its SIM mutants. The Leu150/Asp151/Leu152, Val263/Ser264/Leu265, and Ile317/Asp318/Leu319 were mutated into three consecutive alanine residues, namely, 150-152 SIM, 263-265 SIM, and 317-319 SIM. (C) SUMOylation assay by SUMO-1

of 3D and its selected mutants. K159R/150-152 SIM was generated by mutating Lys159 into Arg159 and Leu150/Asp151/Leu152 into Ala150/Ala151/Ala152. L150A/D151A was created by mutating Leu150/Asp151 into Ala150/Ala151. (D) SUMOylation assay by SUMO-3 of 3D and its selected mutants. Immunoprecipitation and immunoblot analysis were performed with the indicated antibodies in the presence of NEM. Molecular size markers are shown in kilodaltons. SUMO-1 modified Flag-3Ds are depicted by brackets.

Figure 4. Assessments of the relevance of the 3D SUMOylation sites to polymerase activity and virus replication. (A) Schematic representation of the potential lysine residues and SIMs in enterovirus polymerase by sequence alignment. Polyprotein sequences of Enterovirus 71 (GenBank: AB204852.1), Coxsackievirus A16 (GenBank: AY790926.1), Poliovirus (GenBank: KT353719.1), Coxsackievirus A9 (Genebank: D00627.1), Coxsackievirus B3 (GenBank: M16572.1) were used in the alignment. (a) The putative sites of 150-152 SIM and K159. (b) The putative sites of 263-265 SIM. (c) The putative sites of 317-319 SIM and K323. (d) The putative sites of K376 and K427. The SIM motifs are highlighted in red and the lysine residues are in green. (B) An EV71 3D elongation complex crystal structure with a closed conformation active site (PDB entry 5F8J) depicting structural features of the SUMOylation sites. The polymerase adopts an encircled human right hand architecture with thumb (in slate), palm (in grey), and fingers domains surrounding the active site. The fingers domain is further divided into index (in green), middle (in orange), ring (in yellow), and pinky (pink) finger subdomains. The template (in cyan) and product (in green) RNA duplex are shown in a ladder format with the active site nucleotide pair shown as thick sticks. The K159 (side chain in spheres) is within the ring finger subdomain and is an active site residue interacting with the nascent base pair, while the L150 and D151 (side chains in spheres) are on the polymerase surface, being part of the pinky finger. (C, D) *In vitro*

polymerase activity of 3D and its mutants K159R, K159A and L150A/D151A. The time-dependent conversion of the primer P10 to the 14-mer product was compared among WT and three mutant enzymes. Values and error bars shown in panel C were taken from three independent experiments with a representative gels shown in panel B (Student's *t*-test, $*P < 0.05$). (E) Growth curves of EV71 and its mutant IF-L150A/D151A in RD cells. 5×10^5 RD cells were infected with the wild-type EV71 virus or its variant IF-150A/D151A (MOI = 10), and harvested at the indicated times post-infection. Viral growth curves were generated by plotting virus titer (expressed as TCID50/ml) against time. Experiments were carried out in triplicate. Significant differences were determined using the Student's *t*-test ($*P < 0.01$).

Figure 5. In vitro SUMO-1 modification of 3D. (A) Schemes of the gene arrangement of pSUMO-1-Step and pGEX-6p-3D. pSUMO-1-Strep carrying ubc9 (SUMO-conjugating enzyme E2), SAE1, and SAE2 (SUMO-activating enzyme), and SUMO-1 (tagged at the N-terminus with Strep-tag) was used for the expression of the enzymes required for SUMOylation. pGEX-6p-1 carrying 3D was used for the expression of GST-taged 3D. (B) *Escherichia coli* BL21 (pGEX-6p-3D) and BL21 (pSUMO-1-Strep and pGEX-6p-1) were used to produce GST-3D and GST-3D-SUMO-1. The supernatants of the two strains were analyzed by Coomassie blue staining (Lanes 1–3) and immunoblotting (Lanes 4–6) with the anti-3D antibody under the induction of IPTG (500 μM) at 25 °C for 10 h. BL21 (pSUMO-1-Strep and pGEX-6p-1) without IPTG induction was used as the control (Lanes 2 and 5). (C, D) Cell lysates of *E. coli* BL21 (pSUMO-1-Strep and pGEX-6p-1) were subjected to subsequent GST and Strep affinity purification to separate SUMOylated proteins. Fractions during purification of SUMOylated proteins were analyzed by SDS-PAGE and subsequent Coomassie blue staining (C) and immunoblotting (D) by anti-3D and anti-SUMO-1 antibodies. M, marker. Lanes 1–6

of C: crude lysate supernatants, GST column flow through, GST column eluted fraction, dialyzed elution fractions, Strep column flow through, Strep column eluted fraction. Lanes 1–5 of D: crude lysate supernatants, GST column flow through, GST column eluted fraction, Strep column flow through, Strep column eluted fraction. Molecular size markers are shown in kilodaltons. SUMO-1 modified and unmodified GST-3Ds are depicted by brackets and arrows, respectively.

Figure 6. Conjugation of ubiquitin to 3D based on its SUMOylation levels. (A) Ubiquitination assay of 3D and K159R/150-152 SIM. 293T cells were transfected with the indicated constructs. Immunoprecipitation and immunoblot analysis were performed with the indicated antibodies for ubiquitination assay. (B) Ubiquitination and SUMOylation assay of 3D. 293T cells were transfected with the indicated constructs. In particular, HA-UB-KO was co-expressed to remove endogenous ubiquitin, while V5-SENP-1 was co-expressed for deSUMOylation. Immunoprecipitation and immunoblot analysis were performed with the indicated antibodies. (C, D) SUMOylation affected the ubiquitination of 3D in a dose-dependent manner. 293T cells transfected with 2 μg of Flag-3D and 2 μg of HA-Ub or Myc-Ubc9 (0.5, 1, 1.5, and 2 μg) or Myc-SUMO-1 (0.5, 1, 1.5, or 2 μg) or V5-SENP-1 (0.5, 1, 1.5, and 2 μg) in 60 mm dishes. The empty vector was used to adjust the total DNA. Immunoprecipitation and immunoblot analysis were performed with the indicated antibodies. Molecular size markers are shown in kilodaltons. SUMO-1 and ubiquitin modified 3Ds are depicted by brackets.

Figure 7. SUMOylation of 3D increased protein stability. (A) 3D was modified by K63-linked ubiquitin. Flag-3D or K159R/150-152 SIM and HA-K48-Ub or HA-K63-Ub were transfected into 293T cells for ubiquitination assay. Immunoprecipitation and immunoblot analysis were performed

with the indicated antibodies. The ubiquitin modified 3Ds are depicted by brackets. (B, C) Cyclohexamide chase assay of 3D and K159R/150-152 SIM. 293T cells (1×10^5) were transfected with 3D or K159R/150-152 SIM. After 24 h, cells were treated with 100 μg/mL of CHX for the indicated periods of time in the presence or absence of 20 μM MG132. Cell lysates were analyzed by immunoblotting with the anti-Flag antibody. 3D and its mutant bands were quantitated by Image J software. The amount of 3D and its mutant relative to levels in untreated cells was indicated at the bottom of the bands. The plot shows the half-lives of 3D and K159R/150-152 SIM from three independent experiments. Significant differences were determined using the Student's *t*-test (*$P <$ 0.01).

.

Figure 8. SUMO-1 modification promoted EV71 replication. 7×10^6 293T cells were transfected with HA-SUMO-1, Myc-Ubc9 or empty vector in 100-mm dishes. At 24 h post-transfection, cells were infected with EV71 (MOI = 10) for 18 h. One of the dishes with no transfection was used as the control. Immunoprecipitation and immunoblot analysis were performed with the indicated antibodies. (A) SUMOylation and ubiquitination assay of 3D in SUMO-1 elevated cells after EV71 infection by immunoprecipitation. (B) Immunoblot analysis of the cell lysis during infection. Anti-VP1, anti-3D and anti-beta actin antibodies were used to detect the expression of VP1, 3D and beta-actin during infection. Anti-myc antibody was used to detect the expression of Ubc9. SUMO-1 and ubiquitin modified 3Ds are depicted by brackets. 3CD is showed by arrow. (C) Growth curves of EV71 produced from transfected 293T cells in RD cells. 293T cells were transfected with HA-SUMO-1, Myc-Ubc9 or empty vector for 24 h, followed by infection with EV71 at an MOI of 10 for 18 h. Cells were harvested at

indicated time of post-infection to plot the growth curves. Data is presented as the means ± standard deviations obtained from three independent experiments. Significant differences were determined using the Student's *t*-test (*$P < 0.01$).

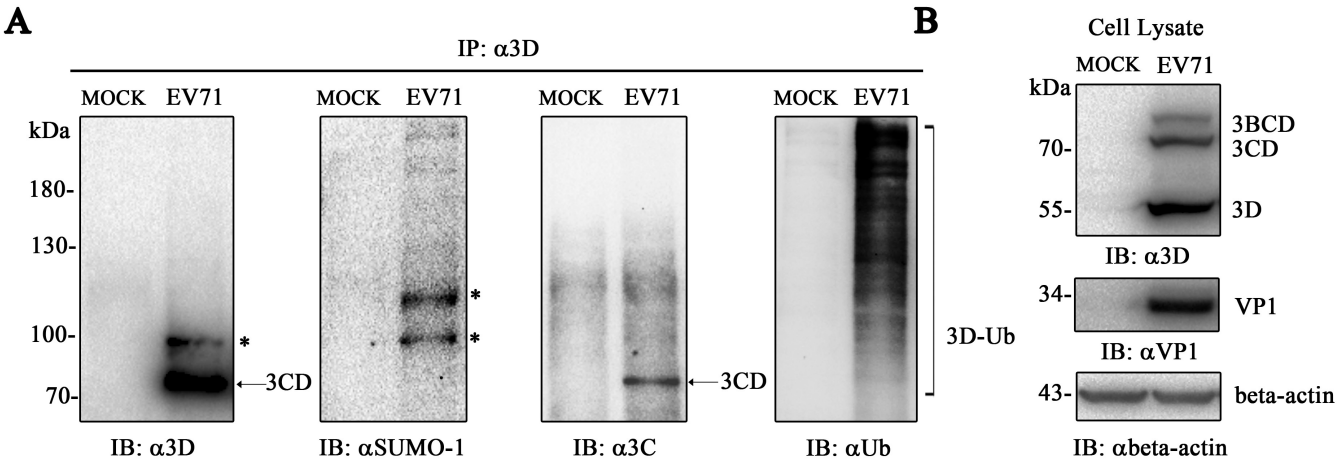

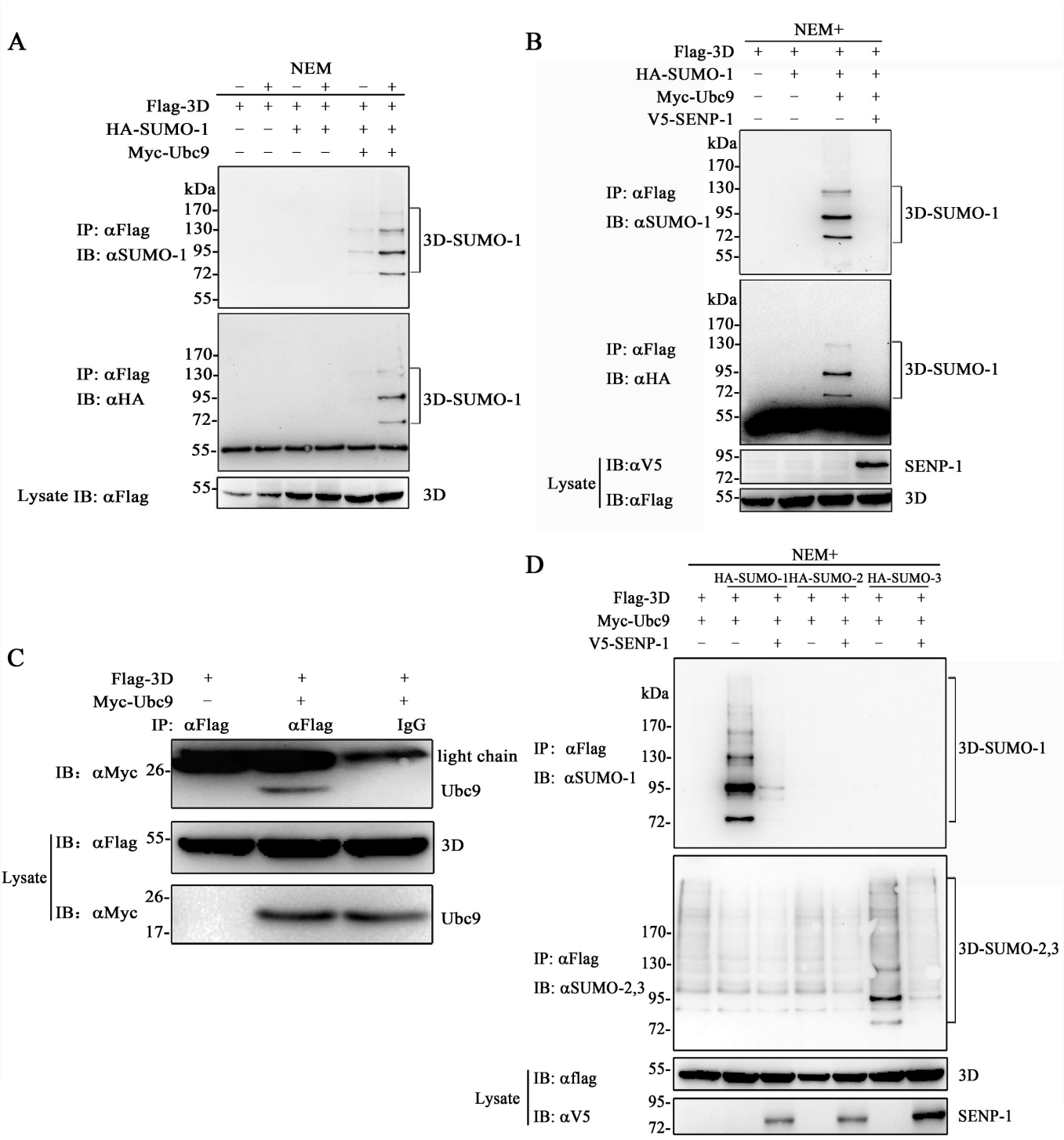

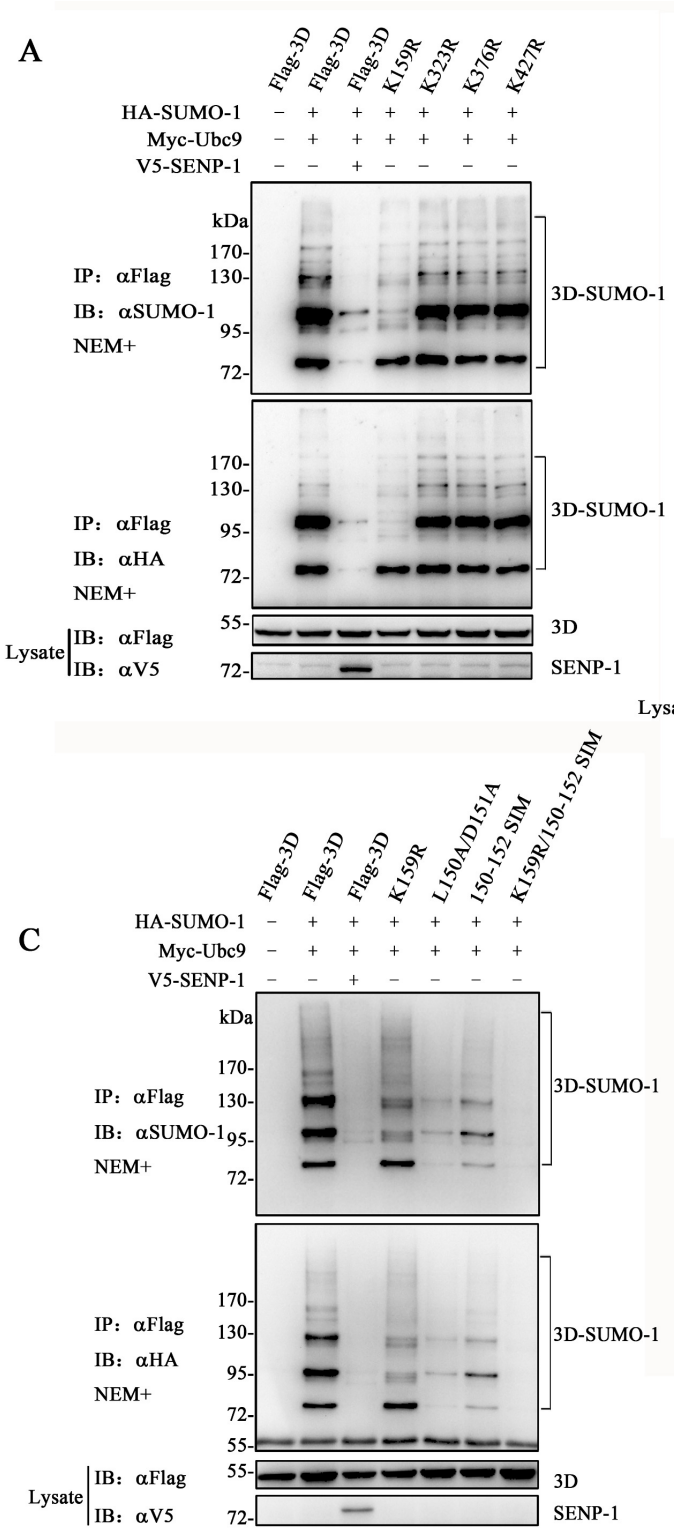

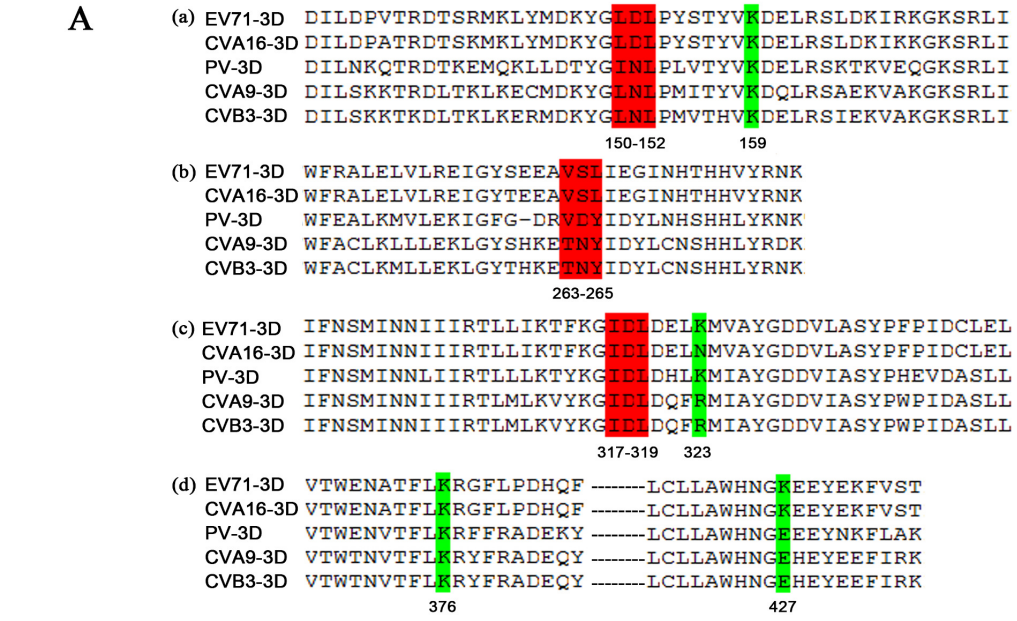

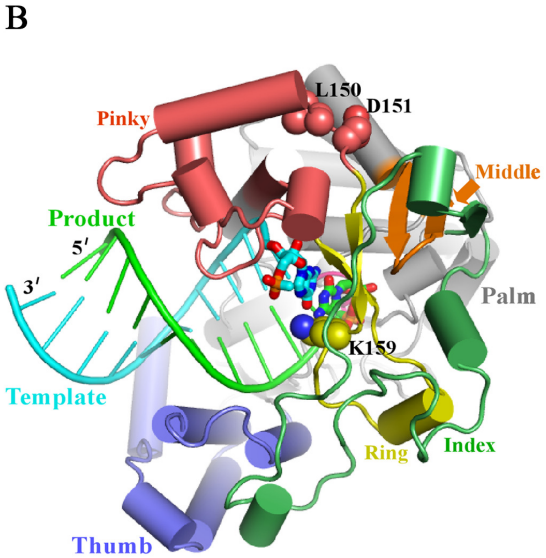

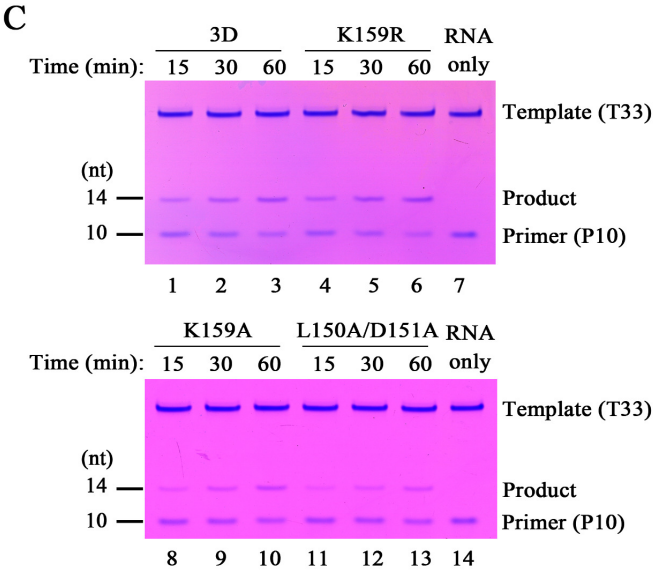

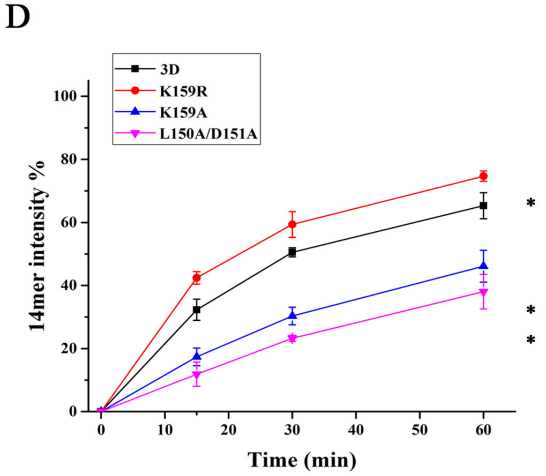

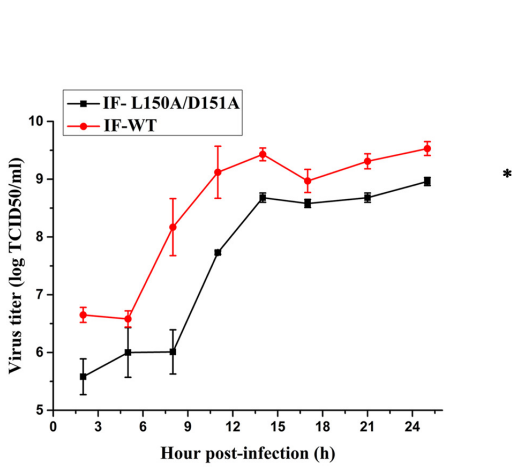

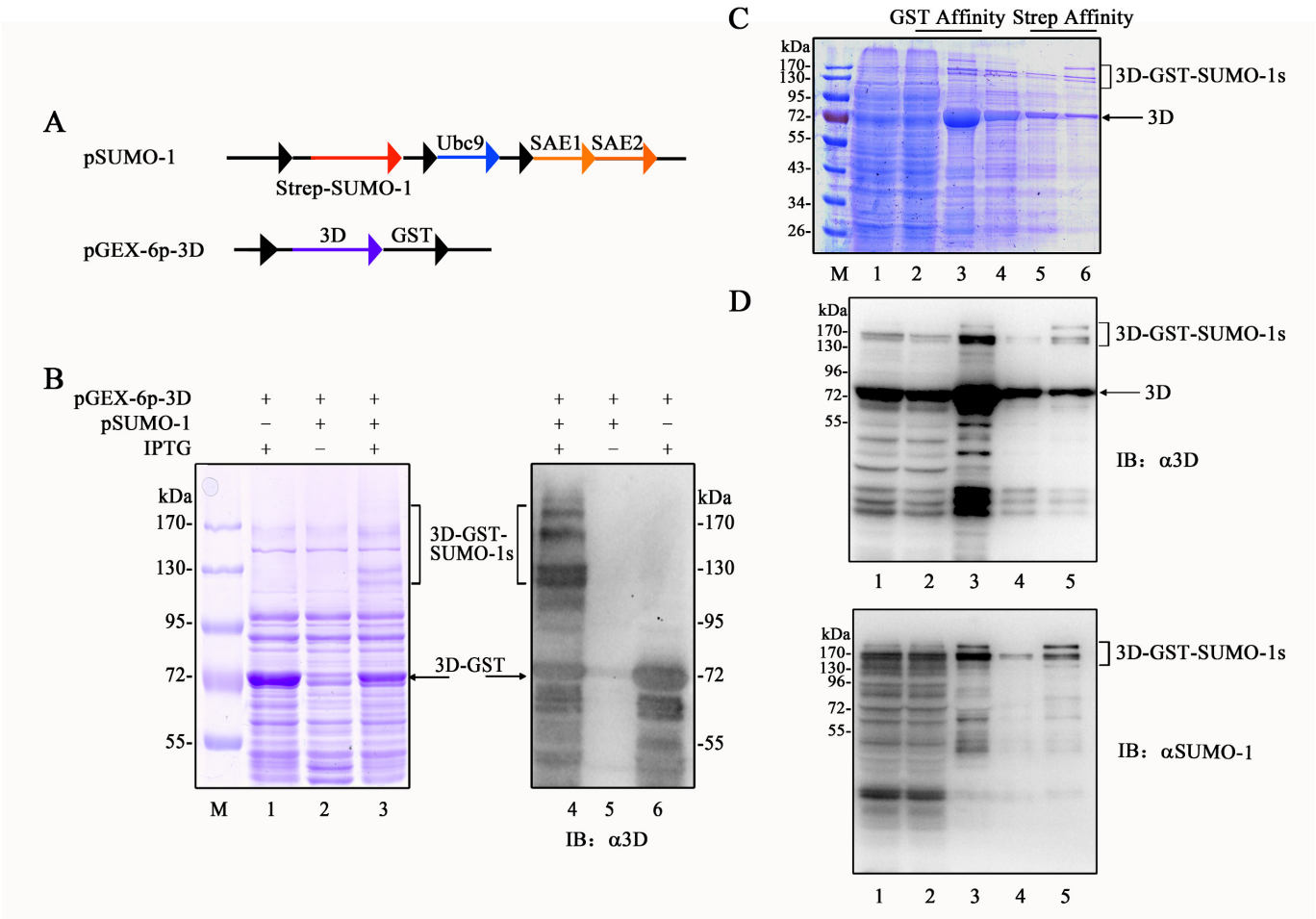

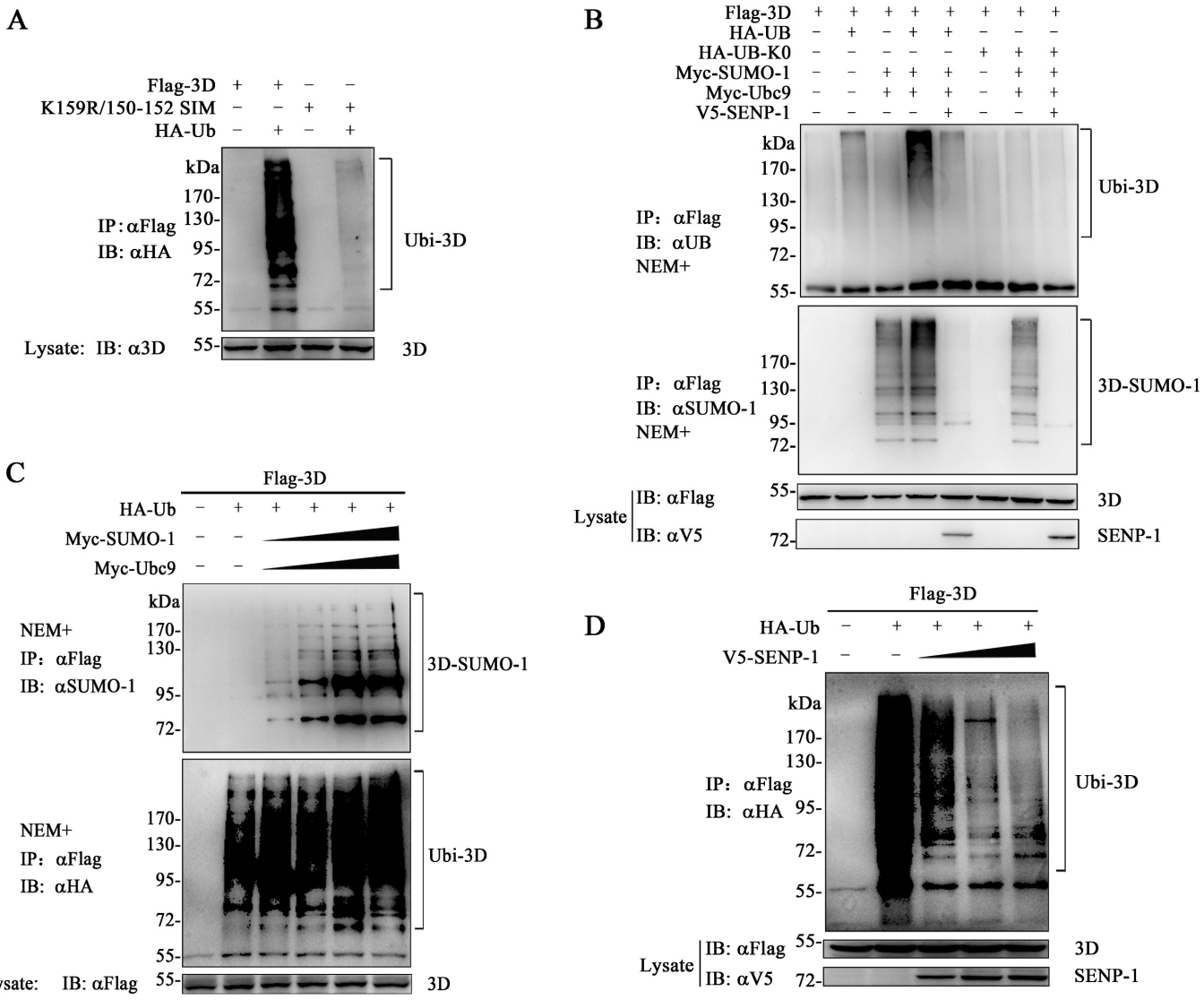

Journal of Virology